Molecular neural crest cell markers enable discrimination of organophosphates in the murine cardiac embryonic stem cell test

R.H. Mennen [a,*], N. Hallmark [b], M. Pallardy [c], R. Bars [d], H. Tinwell [d], A.H. Piersma [a,e]

[a] National Institute for Public Health and the Environment (RIVM), Centre for Health Protection (GZB), Antonie van Leeuwenhoeklaan 9, 3721 MA, Bilthoven, The Netherlands
[b] Bayer AG Crop Science Division, Monheim, Germany
[c] Inflammation, Microbiome and Immunosurveillance, Université Paris-Saclay, Inserm, Châtenay-Malabry, France
[d] Bayer Crop Science, Sophia-Antipolis, France
[e] Institute for Risk Assessment Sciences (IRAS), Utrecht University, Utrecht, the Netherlands

ARTICLE INFO

ABSTRACT

The cardiac embryonic stem cell test (ESTc) originally used the differentiation of beating cardiomyocytes for embryotoxicity screenings of compounds. However, the ESTc consists of a heterogeneous cell population, including neural crest (NC) cells, which are important contributors to heart development *in vivo*. Molecular markers for NC cells were investigated to explore if this approach improved discrimination between structurally related chemicals, using the three organophosphates (OP): chlorpyrifos (CPF), malathion (MLT), and triphenyl phosphate (TPP). To decrease the test duration and to improve the objective quantification of the assay read-out, gene transcript biomarkers were measured on study day 4 instead of the traditional cardiomyocyte beating assessment at day 10. Gene expression profiling and immunocytochemistry were performed using markers for pluripotency, proliferation and cardiomyocyte and NC differentiation. Cell proliferation was also assessed by measurements of embryoid body (EB) size and total protein quantification (day 7). Exposure to the OPs resulted in similar patterns of inhibition of beating cardiomyocyte differentiation and of myosin protein expression on day 10. However, these three chemically related compounds induced distinctive effects on NC cell differentiation, indicated by changes in expression levels of the NC precursor (*Msx2*), NC marker (*Ap2α*), and epithelial to mesenchymal transition (EMT; *Snai2*) gene transcripts. This study shows that investigating NC markers can provide added value for ESTc outcome profiling and may enhance the applicability of this assay for the screening of structurally related test chemicals.

1. Introduction

European legislation for chemical safety necessitates extensive *in vivo* toxicity testing requiring large amounts of laboratory animals. The field of developmental toxicology has been estimated to demand a large part (approximately 65%) of all test animals in Registration, Evaluation, Authorisation and Restriction of Chemicals (REACH) and therefore is a focal area for the development of animal alternatives [1,2]. The cardiac Embryonic Stem cell Test (ESTc) is an often studied animal-free model in developmental toxicology. Originally the ESTc uses the differentiation to beating cardiomyocytes as a screening tool to identify embryotoxic compounds and has been validated by the European Centre for the Validation of Alternative Methods (ECVAM) [3]. However, this assay is known to be limited in various aspects. Therefore, refining this assay

could make it more useful as part of a chemical hazard testing and profiling paradigm.

One of the limitations is the 10-day duration of the test restricting the possibility to use it as a high-throughput screening tool. In addition, the read-out of the test is rather subjective i.e. scoring embryoid bodies (EBs) for beating cardiomyocytes by human eye, using a light microscope. To reduce test duration and to improve the objective quantification of the test results, it is necessary to incorporate alternative and more accurate technologies, such as quantification of the expression of a pre-determined gene transcript set. Quantifying the read-out can improve effect assessment and provide potency rankings between similar chemical structures within the same compound class.

A second limitation is that the standard ESTc protocol only considers beating cardiomyocyte differentiation, effectively ignoring potential

---

effects on any other cell types also present. Neural crest (NC) cell presence in the heterogenous ESTc population has been demonstrated previously in our laboratory, using specific NC markers [4]. By extending the investigations into this cell population within the ESTc, the biological domain of this assay can be better defined and employed. This may enhance the detection of potential embryo-toxicants that do not affect cardiomyocyte differentiation in the ESTc.

This added value of NC cell differentiation related gene expression readouts in the ESTc was explored by testing Organophosphates (OPs), a chemical family with pesticide and flame-retardant applications. Some OPs cause differential developmentally toxic effects in animal models [5]. The mechanism through which the OPs would cause developmental toxicity was long thought to be by specifically inhibiting neuropathy target esterase (NTE) and acetylcholinesterase (AChE) [6]. However, differences in developmental effects observed in rats suggested different mechanisms of action among OPs [6]. Some OPs interact with muscarinic receptors in rats in the nanomolar range as agonists of the m_2 subtype, involved in cardiac contraction [6,7]. Direct effects of some OPs with rat cardiac muscarinic receptors *in vitro* would suggest a potential contribution to cardiac toxicity [7]. The most extensively used OP pesticide is chlorpyrifos (CPF) and acts on cell signalling cascades involved in cardiac and hepatic homeostasis in rats [8].

Exposure of pregnant rats to CPF showed increased degenerated neurons in the cerebellum of the offspring, but also a reduced numbers of Purkinje cells [9]. In neonatal rats, a dose-dependent decrease in muscarinic receptors and reductions in acetylcholine esterase (AChE) were reported [9]. Other studies reported a delay in psychobiological development in neonatal rats when dams were exposed to 1 mg/kg per os [10]. *Farag et al.* [11] described multiple malformations at maternally toxic doses of 25 mg/kg per day, including anophthalmia and ectrodactyly, cleft soft palate, liver haemorrhage, cranial retardation, retardation of pelvic bones, and absence of phalanges. The maternal effects included reduction in body weight and AChE activity [11]. Malathion (MLT) and the flame retardant triphenyl phosphate (TPP) were neither fetotoxic nor teratogenic in rabbits (for MLT) and rats (for TPP) [12,13].

These differences in effect may be attributed to the metabolism of the compounds *in vivo*. CPF and MLT are metabolised to reactive oxon metabolites by hepatic microsomal enzymes [9,14–16]. These oxon metabolites are more potent inhibitors of the AChE enzyme, although there is significant evidence that also other targets are affected by both the parent compounds and metabolites [17–21]. For TPP the parent compound is more reactive and is degraded by hydrolysis into its metabolites diphenyl and monophenyl phosphates by CYP450 enzymes [22,23]. In zebrafish, CPF, MLT and TPP did show a range of teratogenic effects, including cardiac-related developmental defects [20,24–26]. CPF induced pericardial oedema, MLT induced bradycardia and a reduced heart rate [20,25], and TPP impaired cardiac looping and function in the zebrafish model [26]. The variety of developmental effects observed and the proposed mechanisms in different models warrant further investigations within this chemical class.

We studied the OPs CPF, MLT and TPP in the ESTc, specifically for their interference with proliferation, cardiac differentiation, and NC cell development in order to explore the benefit of additional molecular parameters for assessing differential developmental toxicity of structurally related chemicals.

2. Methods

2.1. Test compounds

Chlorpyrifos (CPF, CAS# 2921-88-2), malathion (MLT, CAS# 121-75-5), and triphenyl phosphate (TPP, CAS# 115-86-6) were obtained from Sigma-Aldrich (Zwijndrecht, The Netherlands) and were tested in the subsequent described assays at concentrations up to 330 μM in order to obtain sigmoid-shaped concentration-response curves. 0.25% dimethyl sulfoxide (DMSO, CAS# 67-68-5, Sigma-Aldrich) was used as a solvent.

2.2. Stem cell culture

Murine embryonic stem cells (ES-D3 (D3), ATCC®, Manassas, VA, USA) were cultured as previously described [4,27]. In short, the cells were cultured every 2–3 days in a humidified atmosphere of 37 ℃ with 5% CO_2 by using culture dishes (35 mm, Corning, New York, NY, USA). The culture medium consisted of Dulbecco's Modified Eagle's Medium (DMEM; Gibco, Waltham, MA, USA) enriched with 20% Fetal Bovine Serum (FBS; Greiner Bio-One, Kremsmünster, Austria); 2 mM L-Glutamin (Gibco); 1% Non-Essential Amino Acids (NEAA; Gibco); 1% 5000 IU/mL Penicillin/5000 μg/mL Streptomycin (Gibco); and 0.1 mM β-mercaptoethanol (Gibco). 1000 units/mL leukemia inhibitory factor (LIF; ESGRO®, Millipore, Burlington, MA, USA) was added to the medium to maintain the ES-D3 cells in a pluripotent state.

2.3. Cell viability assay

Cell viability of the ES-D3 cells was executed as before [28]. 500 cells per well were plated in a 96-wells plate (Greiner Bio-One) and were kept warm at 37 ℃ and 5% CO_2 for two hours. Cells were exposed in six replicates to 200 μl of LIF-containing medium including the OPs in concentrations ranging from 330 μM to 0,33 μM or 0 μM or including the negative control penicillin G (500 μg/mL; Sigma-Aldrich), the positive control 5-fluoruracil (0.1 μg/mL; Sigma-Aldrich), or the vehicle control DMSO (0.25%; Sigma-Aldrich). The exposure medium was refreshed at identical final concentrations after three days of exposure under 37 ℃ and 5% CO_2. Following incubation for a further two days, the exposed plates were prepared for the viability fluorescence measurements by replacing 100 μl of solution by 20 μl of CellTiter-Blue reagent (Promega, Leiden, The Netherlands) per well [29]. After 2 h of incubation the extinction values were determined at $544_{Ex}/590_{Em}$ nm on the SpectraMax® M2 spectrofluorometer (Molecular Devices, Berkshire, United Kingdom). Viability levels were calculated relative to the DMSO control (in %). For each test compound the average and standard deviation of the six replicates of each experiment (n = 3) were analysed using PROAST v67.0 as described in section 2.9. This was used to determine the concentration for which 50% of the cells were viable (IC_{50} values).

2.4. Cell differentiation assay

A previously described protocol was used to differentiate the ES-D3 cells into cardiomyocytes during the ESTc assay [3,27]. A similar medium composition was used as for stem cell culture and viability testing except LIF was no longer provided, to enable differentiation. At differentiation day 0, hanging drops were formed by plating a $3.75 \cdot 10^4$ cells/mL suspension in 56 droplets of 20 μl to the lid of a 100/20 mm CELLSTAR® cell culture dish (Greiner Bio-One), which itself held 5 ml of ice-cold phosphate buffered saline (PBS; Ca^{2+}, Mg^{2+} free; Gibco). The hanging drops were kept warm at 37 ℃ and 5% CO_2 for 3 days and were relocated to a 60 mm bacterial petri dish (Greiner Bio-One) with 5 ml of exposure medium. This exposure medium contained concentrations between 330 μM to 0,33 μM of CPF, MLT, TPP or contained controls. After two days of consequent incubation, each embryonic body (EB) was transferred to a well of a culture plate (24-wells, Greiner Bio-One) with 1 ml of exposure medium or controls. Within one experiment, each plate consisted of one condition (= 24 replicates) and was performed in duplicate. On differentiation day 10, after exposing the EBs for an additional 5 days, the EBs were scored for beating cardiomyocytes using a bright field microscope (Olympus BX51, Shinjuku, Japan). The number of beating EBs was divided by the total number of EBs per 24-wells plate. These data were pragmatically used for protein and gene expression analysis in order to determine a concentration at which an effect was measured. To determine such a concentration, two independent experiments were performed for each test compound. The dose for

which beating cardiomyocyte differentiation was inhibited at 50% (ID_{50}) was determined for each compound as described in section 2.9.

2.5. Embryoid body (EB) size measurements

To measure effects on proliferation, EB size and total protein (see section 2.6) were measured as surrogates for proliferation success. The differentiation test was performed as described in the previous paragraph with the same exposure concentrations for the three compounds. To be able to capture one EB with a 4x magnification, EB sizes were measured at differentiation day 7. The EB sizes were captured using a bright field microscope (Olympus BX51, Shinjuku, Japan) and the software CellSens Standard version 2.3 (Olympus Life Science). Measurements were executed by indicating the EB borders using ImageJ 1.51n, which computed the EB area. The average area of 24 EBs per condition was calculated and the 50% effect concentrations (EC_{50} values) were determined as described in section 2.9.

2.6. Total protein measurements

The differentiation test was performed as described in section 2.4 with the same exposure concentrations for CPF, MLT, and TPP. At differentiation day 7, 24 EBs per condition were incubated in cell dissociation buffer (Gibco) at 37 ºC for 3 min. The EBs were collected and after precipitation they were washed with PBS (Ca^{2+}, Mg^{2+} free; Gibco). The EBs were permeabilised in 1 ml of 1% Triton X-100 for 5 min (T9284, Sigma-Aldrich) and protein levels were measured in triplicate using the Micro BCA™ Protein Assay Kit (Thermo Fisher) according to manufacturer's protocol [30]. EC_{50} values were determined as described in section 2.9.

2.7. Protein expression analysis

The differentiation test was performed with exposure to ID_{50} values of each compound determined as described in section 2.9 or with a 0.25% DMSO control. Immunocytochemistry was performed according to a previously described protocol [4]. On differentiation day 5, EBs were collected in 35 mm culture dishes for further differentiation and were later stained using immunocytochemistry on differentiation day 10. The samples were washed with PBS (37 ºC, Ca^{2+}, Mg^{2+} free; Gibco) and were fixed with 4% formaldehyde (Electron Microscopy Sciences, Hatfield, PA, USA) for 30 min at differentiation day 10. For up to 7 days, the fixed cells were kept at 4 ºC until the moment of staining. The cells were washed for 3 x 5 min with PBS (Ca^{2+}, Mg^{2+} free; Gibco) in between each step of the protocol and before and after storage. The EBs were incubated at room-temperature with 0.2% Triton X-100 (T9284, Sigma-Aldrich) in PBS (Ca^{2+}, Mg^{2+} free; Gibco) for 5 min to permeabilise the cells. To minimise non-specific protein binding, samples were incubated with 1% bovine serum albumin (BSA, Sigma-Aldrich) with 0.5% Tween-20 (Sigma-Aldrich) in PBS (Ca^{2+}, Mg^{2+} free; Gibco) for 1 h. The following primary antibodies were added to the EBs in dilution buffer (0.5% BSA, 0.5% Tween-20 in PBS (Ca^{2+}, Mg^{2+} free; Gibco)) at 4 ºC overnight: Activating Enhancer-Binding Protein 2 Alpha (AP2α, early NC marker, sc-12726, Santa-Cruz, 1:100), Myosin Heavy Chain (MF20 (, MAB4470, R&D Systems, 1:100), proliferation marker (Ki67, MA5-14520, Thermo Fisher, 1:500), E-cadherin (ECAD, ECCD-2, 13-1900, Thermo Fisher, 1:1000). The next day, the following secondary antibodies in dilution buffer were added for 1 h: goat-anti-mouse A647 (1:500, A21236, Thermo Fisher), goat-anti-rabbit A488 (1:1000, A11034, Thermo Fisher) or goat-anti-rat A555 (1:500, A21434, Thermo Fisher). A concentration of 1 μg/mL DAPI (Sigma-Aldrich) in dilution buffer was added to the EBs and incubated for 10 min. The EBs were washed with PBS (Ca^{2+}, Mg^{2+} free; Gibco) for 10 min and were covered with a cover glass and mounting medium (Thermo Fisher). The EBs were visualised with a 4x magnification DMi8 microscope (Leica, Germany) with a Leica DFC7000 GT camera (Leica, Germany).

2.8. Gene expression analysis

The stem cells were differentiated until day 4 (24 h of exposure) of the protocol and samples were collected from EBs exposed to ID_{50} concentrations for each compounds determined as described in section 2.9 or to the DMSO control (0.25%). 7 to 8 EB samples in RNAprotect (Qiagen, Cat # 76526) from two independent experiments (n = 2) were stored at −80 ºC. Parallel to this, beating was scored of control plates on differentiation day 10. The stored samples were used for RNA isolation (RNeasy Mini-kit, Qiagen, Cat. # 74104) according to manufacturer's protocol [31]. QIAshredder columns (Qiagen, Cat. # 79654) homogenised the samples and a DNAse step (RNase-Free DNase set, Qiagen, Cat # 79254) was added to the RNA isolation protocol. RNA quantity and quality was assessed using the Nanodrop (Nanodrop Technologies Inc., Wilmington, Delaware) and the 2100 Bioanalyzer (Aligent Technologies, Amstelveen, The Netherlands). Quality control results contained 260 nm/280 nm absorbance ratios between 1.9 and 2.2. RIN (RNA Integrity Number) scores were evaluated >8.2. cDNA was synthesised using a cDNA synthesis kit (Applied Biosystems, Foster City, CA, USA) according to manufacturer's prescriptions. The cDNA was quantified using the thermal cycling conditions: 95 °C for 20 s, followed by 40 cycles of 95 °C for 3 s and 60 °C for 30 s using a 7500 Fast Real-Time PCR system (Applied Biosystems). The used TaqMan® Assays (Thermo Fisher Scientific) are listed in table S1. The relative differences were calculated using the −ΔΔCt method [32], and were normalised against the mean expression levels of the *Hprt1*, *Gusb*, and *Polr2a* housekeeping genes (Table S1). The expression levels for each experiment separately, are provided as supplementary material in figure S1 for experiment 1 and in figure S2 for experiment 2.

2.9. Statistics

The obtained data on cell viability, differentiation, EB size, and protein levels were fitted and statistically analysed using PROAST v67.0 using the exponential method [33]. IC_{50}, ID_{50}, and EC_{50} values were obtained from the concentration-response curves with 90% confidence lower and upper benchmark concentration limit values (BMCL-BMCU). Control values were added to the graphs using a dummy value. An one-way ANOVA test with a post-hoc Sidak's multiple comparisons test ($p < 0.05$) was performed to compare gene expression data to the control samples.

3. Results

3.1. Effects on EB proliferation

The effects of OPs on EB size and total protein content were used as surrogates to determine the *in vitro* concentration provoking a 50% reduction (EC_{50}) in EB proliferation. The EB area (Fig. 1a) and total protein content (Fig. 1b) were reduced by all three OPs in a concentration-dependent manner. For the EB area measurements (Fig. 1a), comparable EC_{50} levels were found, except for MLT which resulted in a lower EC_{50} value where confidence limits did not overlap the values of CPF and TPP (Fig. 1a, Table 1). The total protein measurements resulted in comparable EC_{50} values for all treated groups (fig.1b, Table 1).

3.2. Effects on cell viability and functional cardiomyocyte differentiation

The classical ESTc measures of cell viability and cardiomyocyte differentiation were assessed and compared between the three compounds. Viability was reduced with IC_{50} concentrations for CPF, MLT, and TPP of 85.7 μM, 49.4 μM, and 61.4 μM, respectively (Fig. 2a, b, c, Table 1). CPF, MLT, and TPP reduced the development of beating cardiomyocytes with ID_{50} levels of 117 μM, 73.2 μM, and 143 μM, respectively (Fig. 2d, e, f, Table 1). The overlapping BMC confidence
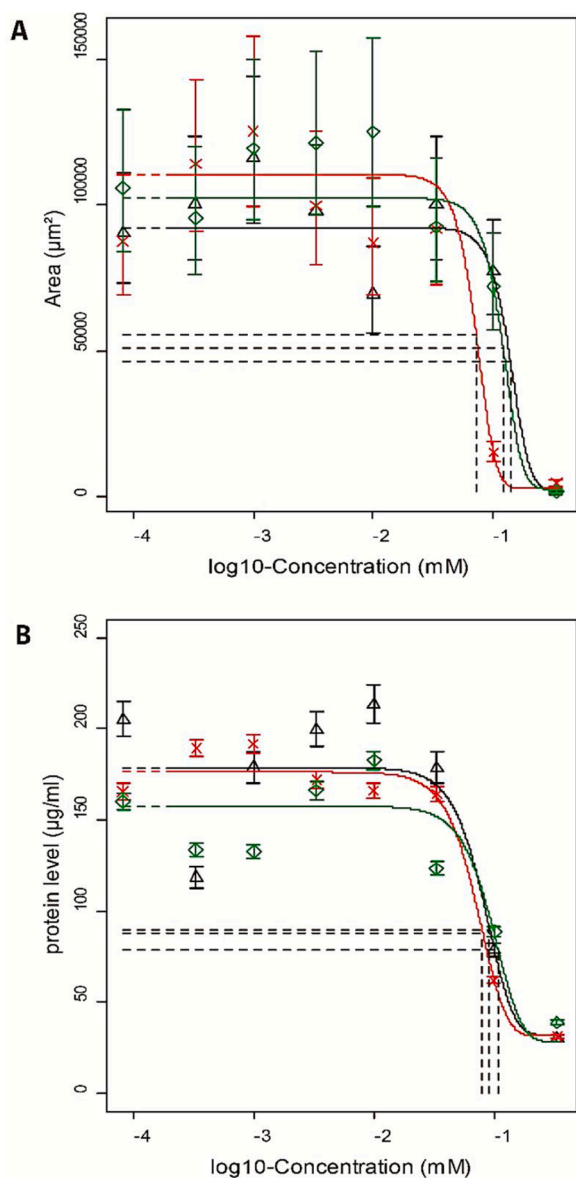
Fig. 1. Concentration-response relationships of CPF, MLT, and TPP on a) EB area and b) total protein content on differentiation day 7. a) EB area expressed in μm^2 for concentrations tested up to 330 μM during differentiation until day 7. The datapoints show the size average of 24 EBs per condition, b) Total protein level expressed in μg/mL for each sample, which consisted of 24 EBs. The datapoints indicate the average of three measurements per sample. Black Δ = CPF, red $\times$ = MLT, green $\lozenge$ = TPP. Control values were indicated at the starting point of each graph and were connected by dotted (coloured) lines to the exposure measurements. Error bars indicate standard deviation. Dotted lines specify the EC_{50} values obtained through statistical analysis using the exponential method of PROAST v67.0 in R (For interpretation of the references to colour in this figure legend, the reader is referred to the web version of this article.).

limits of the three compounds indicated no differences in ID_{50} for inhibition of beating cardiomyocytes or IC_{50} values for cell viability.

3.3. Effects of OPs on protein and gene expression levels

As the classical readouts didn't show differences between the compounds, we needed to zoom in on specific protein and gene expression levels. Effects on proliferation and differentiation were studied with markers for pluripotency, proliferation, cardiomyocyte differentiation, and neural crest cell differentiation. Fig. 3a shows immunostainings for

Table 1
Summary of inhibitory and effective concentrations for the tested endpoints after exposure to CPF, MLT, and TPP. EC_{50}, IC_{50}, and ID_{50} values are indicated in μM with lower and upper BMC confidence limits (BMCL – BMCU).

	Chlorpyrifos	Malathion	Triphenyl phosphate
EB area (EC_{50}); day 7	139 μM (117−162)	72.0 μM (65.3−75.1)	120 μM (106−145)
Protein level (EC_{50}); day 7	92.0 μM (81.6−105)	80.2 μM (75.0−86.1)	108 μM (94.7−129)
Viability (IC_{50})	85.7 μM (42.5−118)	49.4 μM (22.8−105)	61.4 μM (29.9−139)
Differentiation (ID_{50}); day 10	117 μM (74.2−189)	73.2 μM (60.3−73.8)	143 μM (121−168)

proliferation (Ki67), the cardiomyocyte marker myosin heavy chain (MF20), and pluripotency (ECAD) markers after exposure to ID_{50} concentrations of CPF, MLT, TPP (for concentrations used see Table 1) and DMSO (vehicle control). DAPI was used to stain cell nuclei. CPF and MLT exposure showed a more solid DAPI staining within the EBs than controls, whereas TPP exposure affected the round shape of the EBs. Ki67 staining appeared evenly distributed through the EB relative to total amount of cells for all conditions, except for MLT exposure. Staining of MF20 showed clear presence of myosin in all EBs except for the TPP exposed EBs. ECAD staining for pluripotency was present in all exposure groups with staining areas located at different positions within the EB. Fig. 3b indicates presence of the neural crest marker AP2α with clear expression in the MLT and DMSO groups. CPF and TPP exposure did not show a clear AP2α staining.

To assess if the differences between control and treated EBs observed qualitatively at the protein level were also present at the gene transcript level, gene expression analysis was performed for markers of acetylcholine esterase (*Ache*), cell death, pluripotency, proliferation, cardiomyocyte differentiation and neural crest cell differentiation (Fig. 3c, d). Expression for *Ache* seemed to be augmented by CPF and TPP but not by MLT compared to controls, as the two performed experiments showed opposite results in *Ache* expression for MLT as shown in figures S1 and S2 Regarding cell death, the pro-apoptotic marker *Casp3* was statistically significantly downregulated by CPF, but not by TPP and MLT. The expression levels for the necrosis marker *Parp1* were not affected in any of the exposures groups. The pluripotency marker *Ssea-1* showed an upregulated trend in the TPP exposed group and *Cdh1* (=*Ecad*) was statistically significantly upregulated by all three exposure groups. *Ki67* for proliferation showed a downregulated trend in the TPP exposed group and the cardiomyocyte marker *Nkx2−5* showed an upregulated trend in the TPP exposed group. MLT exposure resulted in opposite expression levels in up- or downregulation of *Nkx2−5* when comparing the two experiments, as shown in the supplementary figures S1 and S2.

As to NC markers, *Msx2* showed a downregulated trend in all three exposure groups and the epithelial-to-mesenchymal transition (EMT) marker *Snai2* for NC was statistically significantly upregulated in the CPF and TPP exposed groups when compared to the control.

4. Discussion

The objectives of the experiments conducted in this work were to investigate the added value of molecular gene and protein markers for cell proliferation, cardiomyocyte differentiation, and neural crest (NC) cell development to distinguish between structurally related compounds using the ESTc. Using the organophosphates CPF, MLT, and TPP as model compounds, distinctive effects on gene expression were observed, while effects on cell proliferation and differentiation were not distinctive. At differentiation day 4 (24 h of exposure), gene expression regulation of NC cell markers revealed clear differences between the compounds. Therefore, NC marker gene expression profiles provide
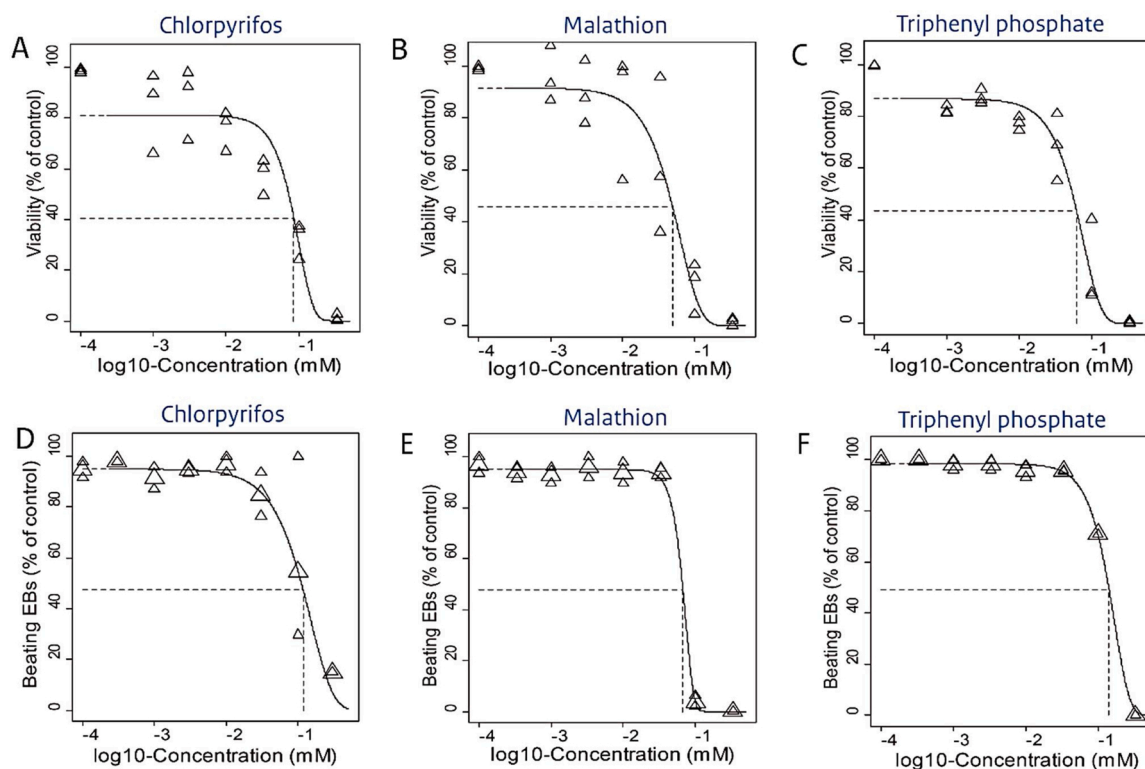
Fig. 2. Cell viability and cardiomyocyte differentiation effects after exposure to CPF, MLT, and TPP. Viability was depicted as relative to the control for a) CPF, b) MLT, and c) TPP and datapoints represent six replicates. Three independent experiments were conducted. The dotted lines specify the IC$_{50}$ values. Effects on differentiation of cardiomyocytes for d) CPF, e) MLT, and f) TPP are expressed in percentage of beating embryoid bodies (EBs) on differentiation day 10 with small triangles as data points and large triangles as average from two independent experiments. The dotted lines specify the ID$_{50}$ values obtained through statistical analysis using the exponential method of PROAST v67.0 in R.

specific developmental toxicity information in addition to the cardiomyocyte beating read-out of the standard ESTc, and so may contribute to the screening and prioritisation of new chemicals for further commercial development.

In particular, the three NC cell specific genes tested did show clear and distinct responses after 24 h of exposure (*Msx2, Ap2α* and *Snai2,* Fig. 3). All three compounds showed a downregulated trend of *Msx2* gene expression. *Msx2* is a neural plate border specifier and a NC precursor gene present in the neural folds [34]. The expression levels of *Ap2α* were upregulated by CPF and MLT (Fig. 3c). AP2α is a NC specifier and alterations in its gene or protein expression affect the non-neural ectoderm, neural plate border, neural folds and in derivatives of the NC cells. These alterations cause defects in NC derivatives in mutant mice [34,35]. Additionally, exposure to TPP and CPF showed a statistically significantly *Snai2* gene transcript upregulation compared to the control. SNAI2 acts as a transcriptional repressor of e.g. E-cadherin and a *Snai2* overexpression would stimulate NC cell delamination and migration by activating epithelial to mesenchymal transition (EMT) when the NC cells separate from the neural tube [34,35]. Although neural tube closure and NC migration akin to *in vivo* morphogenesis cannot occur in the *in vitro* ESTc assay, alterations were observed in the expression levels of NC cell markers after 24 h of exposure (differentiation day 4) to the tested OPs. The presence of NC cells in the ESTc has been investigated in previous research and also showed compound specific effects when testing valproic acid analogues [4]. These previous and current findings confirm the utility of assessing gene expression profiling at an early time-point as part of the toxicity screening with the ESTc [36–38].

The use of a short exposure duration of 24 h for gene expression analysis may also benefit distinguishing developmental effects from possible effects on viability that may arise after longer exposures as shown in Figs. 1 and 2. After 24 h of exposure, the expression levels of *Casp3,* which is a pro-apoptotic gene, were statistically significantly down-regulated following CPF exposure, whereas TPP and MLT did not affect its expression (Fig. 3c). This suggests that the apoptotic pathway is not activated yet at this time-point. The downregulation of pro-apoptotic *Casp3* expression levels was accompanied by an upregulation of the pluripotency marker *Cdh1*. This latter observation illustrates the relationship between increases of highly proliferating pluripotent cells and a relatively lower level of apoptosis. Therefore, monitoring effects on gene expression levels is of added value to the ESTc.

Additionally, a short exposure duration of 24 h benefits NC cell gene expression over cardiomyocyte gene expression. After 24 h TPP exposure, the early cardiomyocyte differentiation marker *Nkx2−5* seemed to be differently expressed, but the late differentiation marker *Myh6* was not expressed yet. In the ESTc, myosin structures start to form on differentiation day 7 [4]. Also on the gene expression level, *Myh6* for myosin is expressed later during development and was most evidently expressed on differentiation day 14 of the embryonic stem cell line HM1 [39].

The effects of the OPs CPF, MLT or TPP specifically on NC cell differentiation have been previously studied to a limited extent. Tussellino et al. (2016) showed developmental defects caused by CPF on anatomical NC derived cranial structures and NC gene expression levels in *Xenopus laevis* [40]. In the chick (*Gallus domesticus*), exposure to a mixture of CPF and cypermethrin (50%; 5%) during embryo development affected the cranial NC cells and resulted in craniofacial dysmorphism [41]. In zebrafish, impairments in cardiac looping and function defects were observed after exposure to TPP [42–47]. Defects in neural crest cell differentiation and migration can cause cardiac deficiencies during embryogenesis, like defective outflow tract septation, abnormal patterning of the aortic arch and great arteries and abnormal
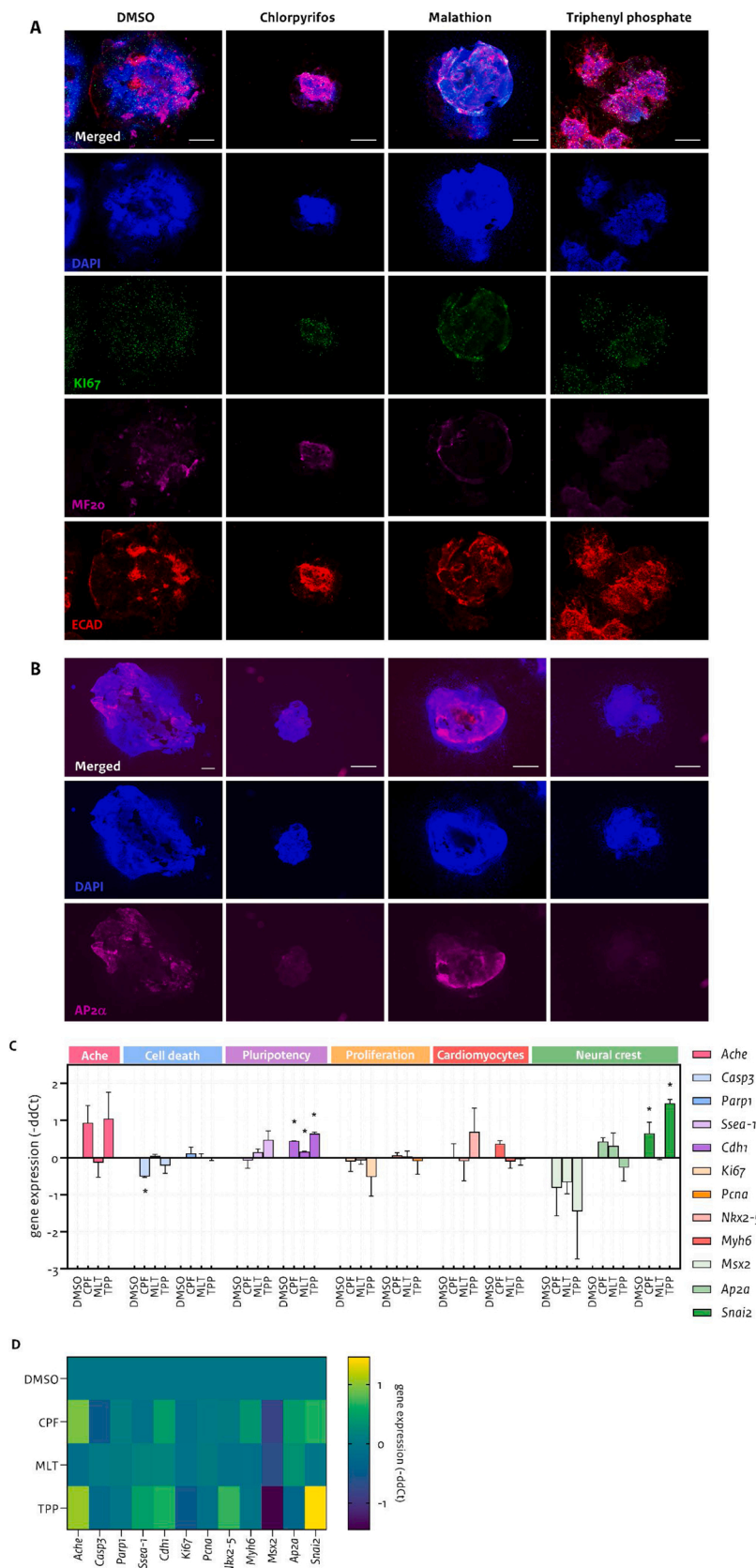
Fig. 3. Effects of CPF, MLT or TPP on the expression levels of markers for Ache, cell death, pluripotency, proliferation, cardiomyocyte differentiation, and neural crest cell differentiation in the ESTc assay. a) Immunocytochemistry staining of the nuclei (DAPI), proliferation marker KI67 (1:500), myosin heavy chain marker MF20 (1:100), and pluripotency marker ECAD (1:1000) after exposure to 0.25% DMSO or ID_{50} concentrations of CPF, MLT and TPP at differentiation day 10 (7 days of exposure). Scale bar indicates 500 μm, magnification 4 × . b) Immunocytochemistry staining of the nuclei (DAPI) and neural crest marker AP2α (1:100) after exposure of 0.25% DMSO or ID_{50} concentrations of CPF, MLT and TPP at differentiation day 10 (7 days of exposure). Scale bar indicates 500 μm, notice the smaller scale bar for the DMSO control for which the image was stitched. magnification 4 × . c) Expression levels of Ache, cell death, pluripotency, ploliferation, cardiomyocyte and neural crest cell related genes after exposure to the ID_{50} concentrations at differentiation day 4 (24 h of exposure). Gene expression was measured using real-time PCR. Error bars indicate the standard deviation. Two independent experiments with in total 7-8 samples. Asterisks indicate a significant difference compared to the DMSO control (one-way ANOVA; Sidak's multiple comparisons post-hoc test). * $p < 0.05$. d) Mean gene expression levels expressed as -ddCt in a heatmap with scale bar ranging from yellow (upregulation) to blue (downregulation) (For interpretation of the references to colour in this figure legend, the reader is referred to the web version of this article.).

cardiac tube looping [48,49].

In contrast to the effects of OPs on NC cell differentiation, the effects on acetylcholine esterase (AChE) have been more extensively studied. OPs inhibit the activity of this enzyme [6,9,11]. In this study, *Ache* gene expression levels seemed to be augmented by CPF and TPP (Fig. 3c). Although an inhibition of *Ache* would be expected, the opposing upregulation of gene expression levels after exposure to CPF has been measured before in embryonic stem cells in conditions where the enzymatic activity was inhibited [15]. Based on the gene expression results in general, TPP seems to be more potent and this may be explained by the lack of metabolic activation within the ESTc. TPP is degraded by hydrolysis into less reactive metabolites diphenyl and monophenyl phosphates by CYP450 enzymes [22,23]. CPF and MLT are metabolised *in vivo* by hepatic microsomal enzymes, belonging to the CYP450 family, to their reactive oxons [9,14–16,50–53]. These metabolites have a higher affinity for AChE in fungicides, although there is significant evidence also other targets are affected that cause adverse effects *in vivo* by both the parent compounds and metabolites [17–21]. In line with most *in vitro* cellular assays, the ESTc has limited xenobiotic metabolic capacity [54,55]. This should be taken into account in *in vitro-in vivo* extrapolations for which the mechanistic boundaries should be further explored [55].

Taken together, our results indicate that adding parameters specific to the neural crest (NC) cell population and gene expression analysis allows discrimination between the tested compounds that is not observable with classical readout parameters usually monitored in the ESTc. Therefore, molecular markers for neural crest differentiation provide a benefit for the detection and discrimination of putative developmental toxicants in the ESTc. In general, this study illustrates the usefulness of more fully exploring and exploiting the biological domain of *in vitro* assays for toxicity screening.

Author statement

Gina Mennen: Investigation, Formal analysis, Writing, Visualisation. **Nina Hallmark:** Supervision. **Marc Pallardy:** Supervision. **Remi Bars:** Supervision, Funding acquisition. **Helen Tinwell:** Supervision. **Aldert Piersma:** Supervision, Conceptualisation.

Conflict of Interest

The authors declare no conflict of interest.

Declaration of Competing Interest

The authors report no declarations of interest.

Acknowledgements

Appendix A. Supplementary data

Supplementary material related to this article can be found, in the online version, at doi:https://doi.org/10.1016/j.toxrep.2021.07.017.

References

[1] A.H. Piersma, Alternative methods for developmental toxicity testing, Basic Clin. Pharmacol. Toxicol. 98 (5) (2006) 427–431.

[2] K. van der Jagt, S. Munn, J. Torslov, J. de Bruijn, Alternative Approaches Can Reduce the Use of Test Animals Under REACH, EC Joint Research Centre, 2004.

[3] E. Genschow, et al., Validation of the embryonic stem cell test in the international ECVAM validation study on three in vitro embryotoxicity tests, Altern. Lab. Anim. 32 (3) (2004) 209–244.

[4] R.H.G. Mennen, J.L.A.J. Pennings, A.H.A. Piersma, Neural crest related gene transcript regulation by valproic acid analogues in the cardiac embryonic stem cell test, Reprod. Toxicol. (Elmsford, N.Y.) 90 (2019) 44–52.

[5] S. Nurulain, M. Shafiullah, Teratogenicity and embryotoxicity of organophosphorus compounds in animal models-a short review, Mil. Med. Sci. Lett. (Voj. Zdrav. Listy) 81 (1) (2012) 16–26.

[6] L.G. Costa, Current issues in organophosphate toxicology, Clin. Chim. Acta 366 (1–2) (2006) 1–13.

[7] M.D. Howard, C.N. Pope, In vitro effects of chlorpyrifos, parathion, methyl parathion and their oxons on cardiac muscarinic receptor binding in neonatal and adult rats, Toxicology 170 (1-2) (2002) 1–10.

[8] A. Meyer, F.J. Seidler, T.A. Slotkin, Developmental effects of chlorpyrifos extend beyond neurotoxicity: critical periods for immediate and delayed-onset effects on cardiac and hepatic cell signaling, Environ. Health Perspect. 112 (2) (2004) 170–178.

[9] E. Commission, Draft Renwal Assessment Report Prepared According to the Commission Regulation (EU) No 1107/2009, Chlorpyrifos, 2017.

[10] B. Laporte, et al., Developmental neurotoxicity in the progeny after maternal gavage with chlorpyrifos, Food Chem. Toxicol. 113 (2018) 66–72.

[11] A.T. Farag, A.M. El Okazy, A.F. El-Aswed, Developmental toxicity study of chlorpyrifos in rats, Reprod. Toxicol. 17 (2) (2003) 203–208.

[12] J.J. Welsh, et al., Teratogenic potential of triphenyl phosphate in Sprague-Dawley (Spartan) rats, Toxicol. Ind. Health 3 (3) (1987) 357–369.

[13] M.G. Machin, W.G. McBride, Teratological study of malathion in the rabbit, J. Toxicol. Environ. Health 26 (3) (1989) 249–253.

[14] E. Commission, Draft Assessment Report (DAR), Malathion, 2004.

[15] C. Estevan, E. Vilanova, M.A. Sogorb, Chlorpyrifos and its metabolites alter gene expression at non-cytotoxic concentrations in D3 mouse embryonic stem cells under in vitro differentiation: considerations for embryotoxic risk assessment, Toxicol. Lett. 217 (1) (2013) 14–22.

[16] X.T. Lu, et al., Cytotoxicity and DNA damage of five organophosphorus pesticides mediated by oxidative stress in PC12 cells and protection by vitamin E, J. Environ. Sci. Health B 47 (5) (2012) 445–454.

[17] J. Gao, et al., Chlorpyrifos and chlorpyrifos oxon impair the transport of membrane bound organelles in rat cortical axons, Neurotoxicology 62 (2017) 111–123.

[18] M.A. Sogorb, et al., Effects of mipafox, paraoxon, chlorpyrifos and its metabolite chlorpyrifos-oxon on the expression of biomarker genes of differentiation in D3 mouse embryonic stem cells, Chem. Biol. Interact. 259 (Pt B) (2016) 368–373.

[19] C. Estevan, et al., Organophosphorus pesticide chlorpyrifos and its metabolites alter the expression of biomarker genes of differentiation in D3 mouse embryonic stem cells in a comparable way to other model neurodevelopmental toxicants, Chem. Res. Toxicol. 27 (9) (2014) 1487–1495.

[20] L.V. Dishaw, et al., Developmental exposure to organophosphate flame retardants elicits overt toxicity and alters behavior in early life stage zebrafish (Danio rerio), Toxicol. Sci. 142 (2) (2014) 445–454.

[21] D.L. Eaton, et al., Review of the toxicology of chlorpyrifos with an emphasis on human exposure and neurodevelopment, Crit. Rev. Toxicol. 38 (Suppl 2) (2008) 1–125.

[22] Q. Zhang, et al., Metabolic mechanism of aryl phosphorus flame retardants by cytochromes P450: a combined experimental and computational study on triphenyl phosphate, Environ. Sci. Technol. 52 (24) (2018) 14411–14421.

[23] Y. Tsugoshi, et al., Inhibitory effects of organophosphate esters on carboxylesterase activity of rat liver microsomes, Chem. Biol. Interact. 327 (2020), p. 109148.

[24] N.A. Ducharme, et al., Comparison of toxicity values across zebrafish early life stages and mammalian studies: implications for chemical testing, Reprod. Toxicol. (Elmsford, N.Y.) 55 (2015) 3–10.

[25] D. Simoneschi, F. Simoneschi, N.E. Todd, Assessment of cardiotoxicity and effects of malathion on the early development of zebrafish (Danio rerio) using computer vision for heart rate quantification, Zebrafish 11 (3) (2014) 275–280.

[26] S.P. McGee, et al., Aryl phosphate esters within a major PentaBDE replacement product induce cardiotoxicity in developing zebrafish embryos: potential role of the aryl hydrocarbon receptor, Toxicol. Sci. 133 (1) (2013) 144–156.

[27] H. Spielmann, et al., The embryonic stem cell test, an in vitro embryotoxicity test using two permanent mouse cell lines: 3T3 fibroblasts and embryonic stem cells, In Vitro Toxicol. 10 (1997) 119–127.

[28] E. de Jong, et al., Potency ranking of valproic acid analogues as to inhibition of cardiac differentiation of embryonic stem cells in comparison to their in vivo embryotoxicity, Reprod. Toxicol. 31 (4) (2011) 375–382.

[29] CellTiter-Blue Cell Viability Assay Technical Bulletin #TB317, Promega Corporation, 2020.

[30] P.K. Smith, et al., Measurement of protein using bicinchoninic acid, Anal. Biochem. 150 (1) (1985) 76–85.

[31] RNeasy Mini Handbook, Qiagen, 2019.

[32] M.W. Pfaffl, A new mathematical model for relative quantification in real-time RT-PCR, Nucleic Acids Res. 29 (9) (2001) e45.

[33] W. Slob, Dose-response modeling of continuous endpoints, Toxicol. Sci. 66 (2) (2002) 298–312.

[34] L.S. Gammill, M. Bronner-Fraser, Neural crest specification: migrating into genomics, Nat. Rev. Neurosci. 4 (10) (2003) 795–805.

[35] M. Simoes-Costa, M.E. Bronner, Insights into neural crest development and evolution from genomic analysis, Genome Res. 23 (7) (2013) 1069–1080.

[36] D.A. van Dartel, et al., Evaluation of developmental toxicant identification using gene expression profiling in embryonic stem cell differentiation cultures, Toxicol. Sci. 119 (1) (2011) 126–134.

[37] D.A. van Dartel, et al., Discriminating classes of developmental toxicants using gene expression profiling in the embryonic stem cell test, Toxicol. Lett. 201 (2) (2011) 143–151.

[38] S.H. Schulpen, et al., Dose response analysis of monophthalates in the murine embryonic stem cell test assessed by cardiomyocyte differentiation and gene expression, Reprod. Toxicol. 35 (2013) 81–88.

[39] S. Rungarunlert, et al., Enhanced cardiac differentiation of mouse embryonic stem cells by use of the slow-turning, lateral vessel (STLV) bioreactor, Biotechnol. Lett. 33 (8) (2011) 1565–1573.

[40] M. Tussellino, et al., Chlorpyrifos exposure affects fgf8, sox9, and bmp4 expression required for cranial neural crest morphogenesis and chondrogenesis in Xenopus laevis embryos, Environ. Mol. Mutagen. 57 (8) (2016) 630–640.

[41] S. Sharma, et al., A combination insecticide at sub-lethal dose debilitated the expression pattern of crucial signalling molecules that facilitate craniofacial patterning in domestic chick Gallus domesticus, Neurotoxicol. Teratol. 76 (2019) 106836.

[42] A. Reddam, et al., mRNA-sequencing identifies liver as a potential target organ for triphenyl phosphate in embryonic zebrafish, Toxicol. Sci. 172 (1) (2019) 51–62.

[43] C.A. Mitchell, et al., Disruption of nuclear receptor signaling alters triphenyl phosphate-induced cardiotoxicity in zebrafish embryos, Toxicol. Sci. 163 (1) (2018) 307–318.

[44] Q. Shi, et al., Developmental neurotoxicity of triphenyl phosphate in zebrafish larvae, Aquat. Toxicol. (Amsterdam, Netherlands) 203 (2018) 80–87.

[45] G.M. Isales, et al., Triphenyl phosphate-induced developmental toxicity in zebrafish: potential role of the retinoic acid receptor, Aquat. Toxicol. (Amsterdam, Netherlands) 161 (2015) 221–230.

[46] Z. Du, et al., Aryl organophosphate flame retardants induced cardiotoxicity during zebrafish embryogenesis: by disturbing expression of the transcriptional regulators, Aquat. Toxicol. (Amsterdam, Netherlands) 161 (2015) 25–32.

[47] S.P. McGee, et al., Aryl phosphate esters within a major PentaBDE replacement product induce cardiotoxicity in developing zebrafish embryos: potential role of the aryl hydrocarbon receptor, Toxicol. Sci. 133 (1) (2013) 144–156.

[48] A. Keyte, M.R. Hutson, The neural crest in cardiac congenital anomalies, Differentiation 84 (1) (2012) 25–40.

[49] T.M. Yelbuz, et al., Shortened outflow tract leads to altered cardiac looping after neural crest ablation, Circulation 106 (4) (2002) 504–510.

[50] X. Wu, et al., From the cover: astrocytes are protective against chlorpyrifos developmental neurotoxicity in human pluripotent stem cell-derived astrocyte-neuron cocultures, Toxicol. Sci. 157 (2) (2017) 410–420.

[51] R.J. Foxenberg, et al., Human hepatic cytochrome p450-specific metabolism of parathion and chlorpyrifos, Drug Metab. Dispos. 35 (2) (2007) 189–193.

[52] J.Y. Khokhar, R.F. Tyndale, Rat brain CYP2B-enzymatic activation of chlorpyrifos to the oxon mediates cholinergic neurotoxicity, Toxicol. Sci. 126 (2) (2012) 325–335.

[53] E. Mutch, F.M. Williams, Diazinon, chlorpyrifos and parathion are metabolised by multiple cytochromes P450 in human liver, Toxicology 224 (1-2) (2006) 22–32.

[54] S. Bremer, et al., Detection of the embryotoxic potential of cyclophosphamide by using a combined system of metabolic competent cells and embryonic stem cells, Altern. Lab. Anim. 30 (1) (2002) 77–85.

[55] M.A. Sogorb, et al., An integrated approach for detecting embryotoxicity and developmental toxicity of environmental contaminants using in vitro alternative methods, Toxicol. Lett. 230 (2) (2014) 356–367.